Journal of Materials Chemistry B

ROYAL SOCIETY OF CHEMISTRY

PAPER

View Article Online
View Journal | View Issue

Cite this: J. Mater. Chem. B, 2024, 12, 8716

Sprayable oxidized polyvinyl alcohol with improved degradability and sufficient mechanical property for fruit preservation†

Yi Lu,‡[ab] Guoming Liu,‡[cd] Kaixin Zhang,[ab] Ziyi Wang,[ab] Peijie Xiao,[ab] Changhua Liu,[ab] Longying Deng,[ab] Fenglu Li,[ab] Gaoxing Pan,[e] Shuxian He,[ab] Jiefeng Gao [f] and Jin Zhang *[ab]

Received 26th April 2024,
Accepted 29th July 2024

DOI: 10.1039/d4tb00896k

rsc.li/materials-b

Besides their limited preservation capacity and low biosafety, traditional fruit preservation procedures exacerbate "white pollution" because they utilize excessive plastic. Herein, an environmentally friendly one-pot method was developed to obtain degradable polyvinyl alcohol (PVA), where the hydroxyl radicals generated through the reaction between hydrogen peroxide (H_2O_2) and iron ions functioned to oxidize PVA. The oxidized PVA (OPVA-1.0) with abundant ketone groups, reduced crystallinity, and short molecular chains was completely degraded into H_2O and CO_2 after being buried in the soil for ~60 days. An improvement in its degradation rate did not weaken the mechanical properties of OPVA-1.0 compared to other modified PVA films because the adverse effect of decreased crystallinity on its mechanical performance was offset by its ion coordination. Alternatively, the tensile strength or toughness of OPVA-1.0 was enhanced due to its internal multi-level interactions including molecular chain entanglement, hydrogen bonding, and metal coordination bonds. More interestingly, OPVA-1.0 was water-welded into various products in a recyclable way owing to its reversible physical bonds, where it was sprayed, dipped, or brushed conformally onto different perishable fruits to delay their ripening by 5–14 days. Based on the cellular biocompatibility and biosafety evaluations in mice, OPVA-1.0 obtained by the facile oxidation strategy was demonstrated to alleviate "white pollution" and delay the ripening of fruits effectively.

1. Introduction

With a rapid growth of population, the problem of food shortage has become increasingly important.[1] One of the main reasons for this situation is that most fresh agricultural products, particularly fruits and vegetables, have highly perishable characteristics and a short shelf life, resulting in nearly half of the products becoming inedible after undergoing the process of picking, transportation, and storage.[2] In China, the serious deterioration of approximately 20–30% of harvested fruits occurs during the agricultural and postharvest stages, leading to significant economic losses before reaching consumers.[3] A variety of factors such as microbial development, oxidation, water loss, aging, and decay affect the shelf life of fruits. In this context, various fruit preservatives have been developed to address the above-mentioned factors, and thus extend shelf life of perishable fruits.[4] However, although these fruit preservation methods extend the shelf life of fruits to a certain extent, some shortcomings that cannot be ignored indeed affect their wide application. For instance, traditional fruit waxing leads to changes in flavor; meanwhile, morpholine and enhancers introduced by wax sealing are harmful to health.[5] Also, the emerging cold chain transportation and controllable gas storage are time-consuming and uneconomical. Finally, the large-scale use of disposable plastic wraps raises new issues of excessive packaging and causes serious environmental pollution problems.[6]

Degradable packaging materials successfully solve the "white pollution" issues of nondegradable petroleum-based materials, while treatments of recycling and centralized composting lead to a sharp increase in the economic cost of these

[a] Qingyuan Innovation Laboratory, 1 Xueyuan Road, Quanzhou 362801, P. R. China
[b] College of Chemical Engineering, Fuzhou University, 2 Xueyuan Road, Fuzhou 350108, P. R. China. E-mail: J_Zhang929@fzu.edu.cn
[c] Shengli Clinical Medical College of Fujian Medical University, 134 East Street, Fuzhou 350001, P. R. China
[d] Department of Orthopedics, South Hospital of Fujian Province, Jinrong South Road, Fuzhou 350028, P. R. China
[e] MOE Key Laboratory for Analytical Science of Food Safety and Biology, College of Chemistry, Fuzhou University, 2 Xueyuan Road, Fuzhou 350108, P. R. China
[f] School of Chemistry and Chemical Engineering, Yangzhou University, Yangzhou 225002, Jiangsu, P. R. China

† Electronic supplementary information (ESI) available. See DOI: https://doi.org/10.1039/d4tb00896k

‡ Y. Lu and G. Liu contributed equally to this work.

degradable materials.[7] Currently, some newly developed modification methods have been proposed for improving the degradation performance of packaging materials, such as blending, cross-linking, and grafting.[8] For instance, Kochkina *et al.* constructed a type of environmentally safe composite film based on maize starch, low molecular-weight chitosan, and polyvinyl alcohol through a blending method, which was demonstrated to possess improved degradability, UV-protective property, and sufficient mechanical performance.[9] However, although blending modification is a simple, low-cost, and effective strategy to improve the degradation performance of packaging materials, there are still some hidden issues that need to be solved. Firstly, low interfacial adhesion, poor dispersibility, and uneven fusion of two or more materials are possible factors deteriorating the mechanical properties of blended polymer systems, where cracks or collapse may occur at the defect or interfacial location during use.[10] Furthermore, blending modification is dependent on the introduction of some easily degradable substances in the non-degradable polymer matrix but does not actually alter the incomplete degradation characteristic of the package materials. For example, blending PVA with naturally degradable materials such as starch, chitosan, and collagen improved the overall degradation rate of the composite membranes, but the PVA molecular chains still existed in their original form during the degradation process.[11] The seemingly accelerated degradation rate of the material was mainly caused by the preferential degradation of the blended biodegradable materials, which then induced the structural collapse of the overall composite membrane.[12]

Thus, improving the degradation performance of polymers and achieving a balance between degradability and mechanical properties have become key scientific issues in constructing ideal packaging materials with wide commercial applications. The introduction of physical effects based on hydrogen bonding, metal coordination bonds, and boric acid bonds is an effective strategy to enhance the mechanical properties of materials.[13] For example, grafting citronellal to the molecular chains of polyvinyl alcohol (PVA) improved its degradation performance significantly; meantime, the further introduction of the hydrophobic humic acid and Fe^{3+} ions resulted in robust mechanical strength due to the high density of hydrogen bonds and coordination interactions.[6] Similarly, the partial disassociation of hydrogen bonds, reassembly of molecular chains, and construction of dynamic Schiff base bonds endowed cellulose with excellent degradability, thermal processability, and sufficient mechanical properties.[14] However, although these crosslinking or grafting modification methods ensure sufficient mechanical properties, while enhancing the degradation behavior of polymers, the large amount of organic solvents employed during the modification process still limits the wide applications of these strategies.[15] Therefore, it is indeed meaningful to find a simple and environmentally friendly modification method simultaneously considering the degradability and mechanical properties of fruit preservation materials.

The strong polarity of PVA endows it with an excellent oxygen-barrier ability, which is an ideal fruit preservation material.[16] For instance, a hybrid membrane composed of PVA, soybean protein isolate, ε-polylysine, and tremella polysaccharide effectively extended the shelf life of and maintained the good quality of blueberries.[17] Additionally, a multifunctional PVA/quaternary ammonium chitosan composite coating was successfully designed, which delayed the senescence of mangoes and papayas significantly.[18] However, although PVA is one of a few fully degradable organic polymers that can be artificially synthesized, it always presents an extremely slow degradation rate of about 8–9% after being buried in natural soil for even 72 days.[19] Specifically, PVA packaging materials have limited degradation ability under natural conditions, which also poses a problem of pollution. Through our in-depth research on the enzymatic degradation process of PVA, we found that currently recognized methods are mainly summarized into the two stages, where step one is related with the oxidization of hydroxyl groups into ketones, and in step two, an aldolase or a diketone hydrolase catalyzes the degradation of PVA.[20] Between them, hydroxyl oxidation is the most challenging stage, always resulting in the poor degradation efficiency of PVA in natural situations, which is currently realized by utilizing an oxidase of PVA, such as a pyrroloquinoline quinone-dependent PVA dehydrogenase (PVA-DH), or an alcohol dehydrogenase from *Lactobacillus kefir* (LK-ADH). Both the PVA-DH and LK-ADH enzymes are present in some specific microorganisms, but these microorganisms are not common in the natural environment.[21] Inspired by this enzyme-catalyzed oxidation mechanism, it is possible to achieve an accelerated degradation rate of PVA in nature by replacing the complex enzyme coordination with chemical oxidation. Meanwhile, to avoid the problem of organic waste liquids generated during the grafting modification process, the products of this oxidation process should be non-toxic and pollution free. More interestingly, the formation of various physical bonds or internal interaction forces should also be considered to ensure the degradation behavior and mechanical properties of PVA package materials.

Jin Zhang

Jin Zhang is currently a Professor in the College of Chemical Engineering at Fuzhou University. She received her BS and PhD degrees from Sichuan University under the supervision of Prof. Zhongming Li. During 2015–2017, she worked as a joint PhD candidate at Harvard Medical School. She was awarded the Young Elite Scientist Sponsorship Program by the China Association for Science and Technology (2023) and Chief Scientist of National Key R&D Program of China (2022). Her research interests focus on smart biomaterials for biodegradable polymers, regenerative medicine, drug delivery, and tissue engineering.

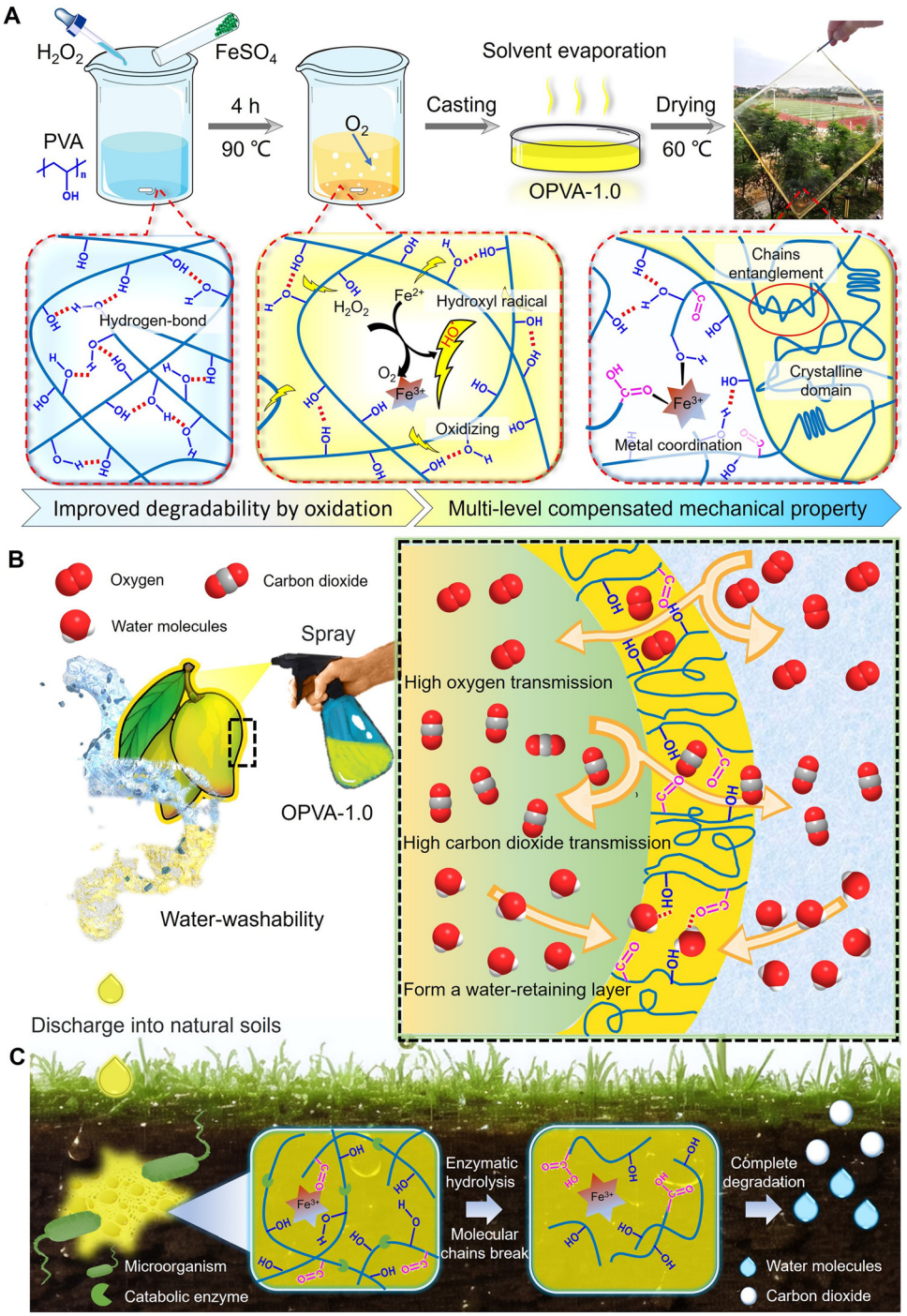

Scheme 1 Synthesis, fruit preservation, and degradation of OPVA. Schematic diagram of (A) oxidized modification process, (B) fruit preservation mechanism, and (C) degradation mechanism of OPVA in natural soil.

Herein, a facile and environmentally friendly modification strategy of PVA is reported, which guarantees its ideal degradation behavior, robust mechanical performance, and fruit preservation performance simultaneously. As shown in Scheme 1(A), the hydroxyl radicals generated during the Fenton reaction of H_2O_2 and divalent iron ions were utilized to oxidize the hydroxyl groups in the PVA molecular chains into ketone compounds, accelerating the following enzymatic degradation process. Moreover, iron ions as reducing agents formed dynamic coordination with the hydroxyl and carboxyl groups on the oxidized polyvinyl alcohol (OPVA) molecular chains, which combined with molecular chain entanglement and hydrogen bonding effect to maintain sufficient mechanical properties in the OPVA material based on these internal multi-level interactions. OPVA could be sprayed on the surface of fruits to form a uniform plastic wrap quickly, and this "spray-type" cling film was demonstrated to delay the ripening of

fruits by 5–14 days. Ultimately, the improved O_2 transfer rate and promoted CO_2 release inhibited the anaerobic respiration of the fruits, and a large amount of hydroxyl groups on the OPVA membrane captured the moisture generated by respiration to also guarantee the freshness of the fruits (Scheme 1(B)). Considering that was possible to drip the OPVA solution into the soil during the spraying or the washing process, we also conducted a degradation performance test to verify whether it will cause plastic pollution in the natural environment. It was interesting to verify that our modified OPVA-1.0 was almost completely degraded within 60 days under natural conditions. The ketone groups generated after the oxidative modification were more easily degraded by microorganisms; meanwhile, microorganisms promoted the decomposition of the OPVA molecular chains into small segments through the released degradation enzymes (Scheme 1(C)). Overall, our proposed PVA modification method is undoubtedly a strategy of killing two birds with one stone, which not only realizes the degradation of PVA under natural conditions, but also provides a new type of functional coating for fruit preservation.

2. Experimental

2.1. Materials

Polyvinyl alcohol (PVA-1099, weight-average molecular weight M_w = 64 000 g mol^{-1}) was provided by Yong'an Baohualin Industrial Development Co., Ltd (Fujian, P. R. China). Ferrous sulfate heptahydrate (AR $\geq$ 99.0%) was obtained from Greagent Co., Ltd (Shanghai, P. R. China). 30% H_2O_2 was purchased from Sinopharm Chemical Reagent Co., Ltd (Shanghai, P. R. China). Phosphate buffer saline (PBS, 0.01 M, pH 6.8) was purchased from Yuanye Biotechnology Co., Ltd (Shanghai, P. R. China). Fetal bovine serum and Dulbecco's modified Eagle medium (RPMI-1640) were provided by American Gibco (Gaithersburg, MD, USA). Penicillin–streptomycin was purchased from Thermo Fisher Scientific Inc. (Waltham, MA, USA). Cell Counting Kit-8 (CCK-8) was acquired from Dojindo Laboratories (Kumamoto, Japan). All chemicals were used as received without further purification.

2.2. Fabrication of OPVA polymer and OPVA coating solution

Firstly, 3.0 g of PVA was dissolved in 25.0 mL of deionized water with continuous stirring at ~90 °C for 2 h. Subsequently, 30% hydrogen peroxide (H_2O_2; 0.5, 1.0, 1.5 mL) and 0.003 mg mL^{-1} ferrous sulfate solution ($FeSO_4$; 1.0 mL) were added dropwise to the PVA solution in turn with stirring at ~90 °C for another 4 h. Finally, the above-mentioned solution was poured slowly into a culture dish and dried at 60 °C for 24 h. The defect-free film was manually peeled off from the culture dish and the OPVA-0.5, OPVA-1.0, and OPVA-1.5 groups represent the OPVA samples with different H_2O_2 volumes of 0.5, 1.0, and 1.5 mL, respectively.

The OPVA solution could be sprayed, dipped, and brushed onto diverse fruits to form a thin coating. Firstly, 3.0–8.0 g of the above-obtained films was dissolved in 30.0 mL of deionized water using a magnetic stirrer at 60 °C for 1 h. Then, the solution was coated onto different fruits after being cooled at room temperature for 20 min. For example, the spraying method was employed for bananas, the dipping method was used for strawberries and tomatoes used, and the brushing method was used mango.

2.3. Characterization

The chemical structure of the oxidized polyvinyl alcohol (OPVA) film was investigated by Fourier-transform infrared spectroscopy (FT-IR, Spectrum 100, PerkinElmer, Waltham, MA, USA). The scan range was set from 4000 to 400 cm^{-1} with a resolution of 0.5 cm^{-1}. X-ray photoelectron spectroscopy (XPS) was performed using a K-Alpha X-ray Photoelectron Spectrometer System (Thermo Scientific, USA) with a monochromatic aluminium source (Al Kα = 1486.6 eV) for X-ray excitation. The operating voltage and current were set as 12 kV and 6 mA, respectively, and the core-level and survey spectra were measured with pass energies of 150.0 eV and 1000.0 eV, respectively. The standard C1s peak located at 284.6 eV was used as the reference. The molecular weight and its distribution were determined by gel permeation chromatography (GPC, Malvern, GPCmax TDA305, UK) using 0.1 M sodium nitrate as the eluent. The system was operated at a solvent-flow rate of 0.7 mL min^{-1} in a Viscotek A6000M column with a size of 300.0 × 8.0 mm^2 at 40 °C, and the method was established with PEO 24k as the narrow scale and validated with dextran 73k as the wide scale. The light transmittance test was carried out on an ultraviolet-visible (UV-vis) spectrophotometer (UV-3600i Plus, Shimadzu, Japan) in the wavelength range of approximately 300–800 nm. The sample was cut into strips with a width of 10.0 mm and a length of 30.0 mm for assessing its transparency. Viscosity data was collected using a rheometer (MCR-302, Anton Paar, Austria) with a 25-mm cone and plate geometry with a 0.1-radian cone angle. The rheological behavior of the OPVA solution was measured under ambient conditions in shear mode at shear rates in the range of 10^{-2} to 10^2 s^{-1}. *In situ* X-ray diffraction measurement was performed using an Ultima IV diffractometer (Rigaku, Japan) with an incident X-ray wavelength of 1.54 Å. The operating voltage and current were set as 40 kV and 30 mA, respectively, and the measurements were performed in the 2θ range of 5°–90° with a scan speed was 15° min^{-1}. The thermogravimetric-differential scanning calorimetry (TGA) analysis of all the samples was performed using an SDT Q600 (TA Instruments, USA) at a heating rate of 10 °C min^{-1} under a constant air flow rate of 100.0 mL min^{-1}.

2.4. Differential scanning calorimetry measurement

Differential scanning calorimetry (DSC 214, NETZSCH, Germany) was performed to assess the crystallization behaviors of the different film samples. For the DSC measurement, the samples were first heated from 60 °C to 230 °C at a heating rate of 10 °C min^{-1} in a nitrogen atmosphere with a flowing rate of 30 mL min^{-1}. Then, the crystallinity of the film samples (χ_{sample}) was calculated using the following equation:

$$\chi_{sample} = \frac{H_{sample}}{\Delta H_m^\circ} \quad (1)$$

where ΔH_m° is the enthalpy of fusion for 100 wt% crystalline

PVA (161 J g^{-1}) and H_{sample} is the melting enthalpy of the crystalline domains per unit mass of sample.[22]

2.5. Small angle X-ray scattering tests

The structures of the films under stretching were analyzed by two-dimensional (2D) small-angle X-ray scattering (SAXS) with a wavelength of 0.103 nm using beamline BL16B of the Shanghai Synchrotron Radiation Facility (SSRF).[23] A Mar 165 CCD detector (2048 × 2048 pixels with a pixel size of 80 mm) was used to collect 2D SAXS patterns and the distance between the sample and the detector was set as 2.0 m. The data acquisition time was 20 s, with an exposure time of 15 s for each frame. The Fit2D software from the European Synchrotron Radiation Facility was used to analyze the data. The SAXS data was corrected for background scattering through air and a KI/I_2 solution, and the 2D SAXS patterns were integrated azimuthally to obtain the 1D scattering profiles using the following formula:

$$q = \frac{4\pi \sin\theta}{\lambda} \quad (2)$$

where q is the module of the scattering vector, λ is the X-ray wavelength, and 2θ is the scattering angle.

The average distance (L) between the crystalline domains was calculated from the one-dimensional integrated SAXS curves according to Bragg's law, as follows:

$$L = \frac{2\pi}{q_{max}} \quad (3)$$

where q_{max} is the critical vector corresponding to the highest peak intensity.[24]

2.6. Mechanical performance

The mechanical properties of OPVA were measured using a texture analyzer (SMS, Ltd Hamilton, MA, USA) at room temperature. The samples were placed at room temperature for a period of time to reach a water-absorption equilibrium state, as revealed from by the unchanged sample mass. Each sample was cut into rectangular pieces with a dimension of 30.0 × 5.0 × 0.2 mm^3 and the stretching rate was set as 1.0 mm s^{-1} for tensile test until rupture. The Young's modulus was calculated according to slope of the linear region in the stress–strain curves and toughness was calculated by integrating the area enclosed by the curves. At least three parallel sample measurements were performed to obtain the average values.

2.7. Degradation evaluation

To evaluate the degradability of the different PVA and OPVA films, a soil burial test was performed according to previously reported protocols.[14] Firstly, samples with certain weights were cut into 1.0 × 1.0 cm^2 pieces and buried in soil to a depth of ~5 cm in a garden at Fuzhou University. Afterwards, the films were taken out at predetermined intervals (day 7, 14, 21, 28, 60, and 90) and gently washed with water to remove the adhered soil. The dry weights of all the samples were measured carefully and the degradation rates of the films were calculated depending on the weight loss of the samples over time. At least three parallel experiments were conducted for each group to obtain convincing results, and the weight loss value as a function of time was calculated using eqn (4) as follows:

$$\text{Weight loss } (\%) = \frac{W_0 - W_t}{W_0} \times 100\% \quad (4)$$

where W_0 and W_t represent the initial weight when purchased and real-time weight in subsequent days after purchase, respectively.

Visual observations were also recorded using a mobile phone and fluorescence microscope (BDS400-FL, Aote Optical Instrument Co., Ltd, Chongqing, China). In the case of the samples with low weight loss, their surface was cleaned with water, and then photographed, while in the case of some samples with obvious degradation behavior (especially at 28 days), photography was directly utilized because of the difficulty in cleaning and removing surface soil sediment.

2.8. Permeabilities of water vapor, oxygen, and carbon dioxide assay

The steady-state water vapor permeability was measured using a water vapor transmission rate tester (W3/031, Labthink, Jinan, China). Circular samples with a diameter of 10 mm were precisely cut using a knife and used as test specimens. This experiment was performed at 23 °C ± 1 °C with a high relative humidity of 86% ± 1%. The amount of water vapor transferred from the surrounding air through the film was calculated and expressed as WVTR in g $(m^2\ 24\ h)^{-1}$.

The O_2 and CO_2 permeabilities of the films were determined using a Gas Permeation Analyzer (VAC-V2, Labthink, Jinan, China) at 50% relative humidity and 23 °C. The films were humidified for 1 min using an Electro Tech Ultrasonic Humidification System (Glenside, PA) operated at 100% relative humidity for easy handling. The films were cut into squares of approximately 10.0 × 10.0 cm^2, and the test cell for the Labthink VAC-V2 was over 50 cm^2 area of the film.

2.9. Fruit preservation evaluation

The fruit weight was recorded daily using an electronic weighing scale. The weight loss rate of the fruits was defined as the ratio of weight loss to the initial weight. The firmness of a strawberry was determined using a texture analyzer (SMS, Ltd Hamilton, MA, USA) with a compression probe (P/2.5R), where the testing speed and compression strain were predetermined to be 1.0 mm s^{-1} and 40%, respectively. The strawberry was placed in the middle of the probe and the results are presented as the peak force. At least three parallel samples were performed to obtain the average values.

2.10. Biocompatibility evaluation *in vitro*

The mouse embryonic fibroblast cell line NIH/3T3 was employed to investigate the *in vitro* biocompatibilities of the PVA, OPVA-0.5, OPVA-1.0, and OPVA-1.5 films. All the cells were cultured with Dulbecco's modified Eagle's medium (DMEM) containing 10.0% (V/V) fetal bovine serum and 0.1% (V/V) penicillin–streptomycin in a saturated humidity incubator with 5% CO_2 at 37 °C. Prior to the cell culturing work, all the

samples were initially cut into rectangular pieces with a size of $15.0 \times 15.0 \times 0.3$ mm^3, disinfected with 75% (V/V) ethanol, and sterilized by ultraviolet light irradiation for 1 h in each side. Then, all the films were soaked in 20.0 mL of DMEM medium at 4 °C for 24 h to acquire the extract solutions of the PVA, OPVA-0.5, OPVA-1.0, and OPVA-1.5 films. Extracts of the samples in the same concentrations were added to the cell culture medium and incubated with the cells for 1, 3, and 5 days. The cell viability was quantitatively evaluated using the CCK-8 method. In detail, the LO2 and NIH/3T3 cells were directly cultured in an extracting medium at a density of 1.0×10^3 cells mL^{-1} in a 96-well cell culture plate. After being cultured for 1, 3, and 5 days, the culture medium was pumped and 0.1 mL of 10% (V/V) CCK-8 working solution was added. After being incubated at 37 °C for 30 min away from light, the absorbance of the specimens at 450 nm was measured using an H4150 spectrophotometer (Epoch, BIO-TEK, Winooski, VT, USA). The growth status of the cells cultured in fresh DMEM medium was used as the control group and at least three samples for each group were performed and the results are presented as mean ± SD.

Besides, live/dead staining images were also obtained for evaluating the *in vitro* biocompatibilities of the PVA, OPVA-0.5, OPVA-1.0, and OPVA-1.5 films qualitatively. The NIH/3T3 and LO2 cells at a density of 1.0×10^4 cells per well were cultured in 24-well plates. After 24 h of incubation, the cells were treated with extract solutions of the PVA, OPVA-0.5, OPVA-1.0, and OPVA-1.5 films in 5% CO_2 at 37 °C for 1, 3, and 5 days. Then, the cells were washed with PBS thrice, followed by being incubated with 10 μL of calcein acetoxymethyl ester and 15 μL of propidium iodide solutions at 37 °C for 15 min. Finally, the cell morphology and amount were observed using an inverted fluorescence microscope (Leica DMI 6000B, Germany). All experiments were performed in triplicate.

2.11. Biosafety evaluation *in vivo*

For the *in vivo* biosafety tests, mice (6–7 weeks) were purchased from Beijing Vital River Laboratory Animal Technology Co., Ltd (Beijing, China). The mice were fed with an aqueous OPVA solution in a period of 21 days to investigate its biosafety impact on mammalian health. Briefly, 0.1 mL of the OPVA solution (0.5, 2.5, and 5.0 mg mL^{-1}) was given once daily by oral gavage. After continuous feeding for 21 days, all the mice were euthanized, and then their visceral organs (including heart, liver, spleen, lung, and kidney) were collected for histological analysis. Specifically, the harvested visceral organs were immersed in 4% paraformaldehyde, decalcified in ethylenediaminetetraacetic acid (pH = 7.2), dehydrated with ethanol, and finally embedded in paraffin. H&E staining images were obtained by employing an inverted fluorescence microscope (Leica DMI 6000B, Germany) to observe three different regions from the same section. To analyze WBC, Neu, Lym, Mon, Eos, Bas, RBC, and PLT as indicators of the proper functioning of organisms, the blood was further placed in an anticoagulant tube and sent to Wuhan Sevier Biotechnology Co., Ltd. All animal experiments were executed according to the protocols approved by the Institutional Animal Care and Use Committee of Fuzhou University, and the experimental procedures were in agreement with the guide for the care and use of laboratory animals (Ministry of Science and Technology of China, 2006).

2.12. Statistical analyses

All the data collected in this work are presented as mean ± standard deviation (SD). The SPSS 13.0 statistical software was used to analyze the data by one-way analysis of variance (ANOVA). $^*P < 0.05$, $^{**}P < 0.01$, and $^{***}P < 0.001$ were defined as significant for all statistical tests.

3. Results and discussion

3.1. Successful synthesis of OPVA

The samples employed in the current study were obtained from oxidation of PVA through Fenton reactions between H_2O_2 and Fe^{2+} ion. As shown in Fig. 1(A), H_2O_2 was reacted with Fe^{2+} ions to generate Fe^{3+} ions and hydroxyl radicals ($^\bullet$OH), and then $^\bullet$OH successfully oxidized the hydroxyl groups on the PVA molecular chains into ketone groups.[25] The production of ketone groups disrupted the orderly arrangement of the PVA molecular chains and effectively reduced their cohesion forces, thereby endowing OPVA with a relatively fast degradation rate.[26] Based on the different volumes of introduced H_2O_2 (0.5, 1.0, and 1.5 mL) during oxidation, the oxidized PVA sample was defined as OPVA-0.5, OPVA-1.0, and OPVA-1.5, respectively. The successful oxidation of PVA was confirmed by Fourier-transform infrared (FT-IR) spectroscopy (Fig. 1(B)). The FT-IR spectrum of OPVA showed new characteristic peaks in the range of 1717–1588 cm^{-1}, which were assigned to the C=O stretching vibrations caused by the oxidation of the hydroxyl groups on the PVA chains.[27] In addition, the position of the hydroxyl groups was red-shifted, as revealed in the FT-IR spectrum, which was ascribed to the coordination interactions between the hydroxyl groups and ferric trivalent irons.[28] As displayed in Fig. 1(C) and Fig. S1 (ESI†), the presence of C1s and O1s indicated that the membrane composition was not changed after modification; meanwhile, the corresponding peaks of generated Fe^{3+} were not observed due to their amount lower than the detection limit of X-ray photoelectron spectroscopy (XPS). By further peak fitting treatment of C1s, the C–C and C–O in the PVA gradually changed into C=O in OPVA with an increase in H_2O_2 content, further proving that the addition of H_2O_2 and ferrous iron oxidized the PVA molecules, and consequently generated carbonyl compounds.[29]

Thermal stability is a major concern for materials to be used in a wide range of applications. As shown in Fig. 1(D), the thermogravimetric analysis (TGA) curves mainly presented three stages, as follows. Firstly, there was an approximately 10% mass loss in the PVA and OPVA films as the temperature increased to 220 °C due to the evaporation of free moisture within the film. Then, because of the dehydration of the hydroxyl groups in the polymer chains and the degradation of the polymer backbone, both the PVA and OPVA samples lost 60–70% of their mass. Compared with PVA, the lower hydroxyl content in OPVA led to a lower loss due to hydroxyl dehydration. In addition, Fe^{3+} formed coordination with the

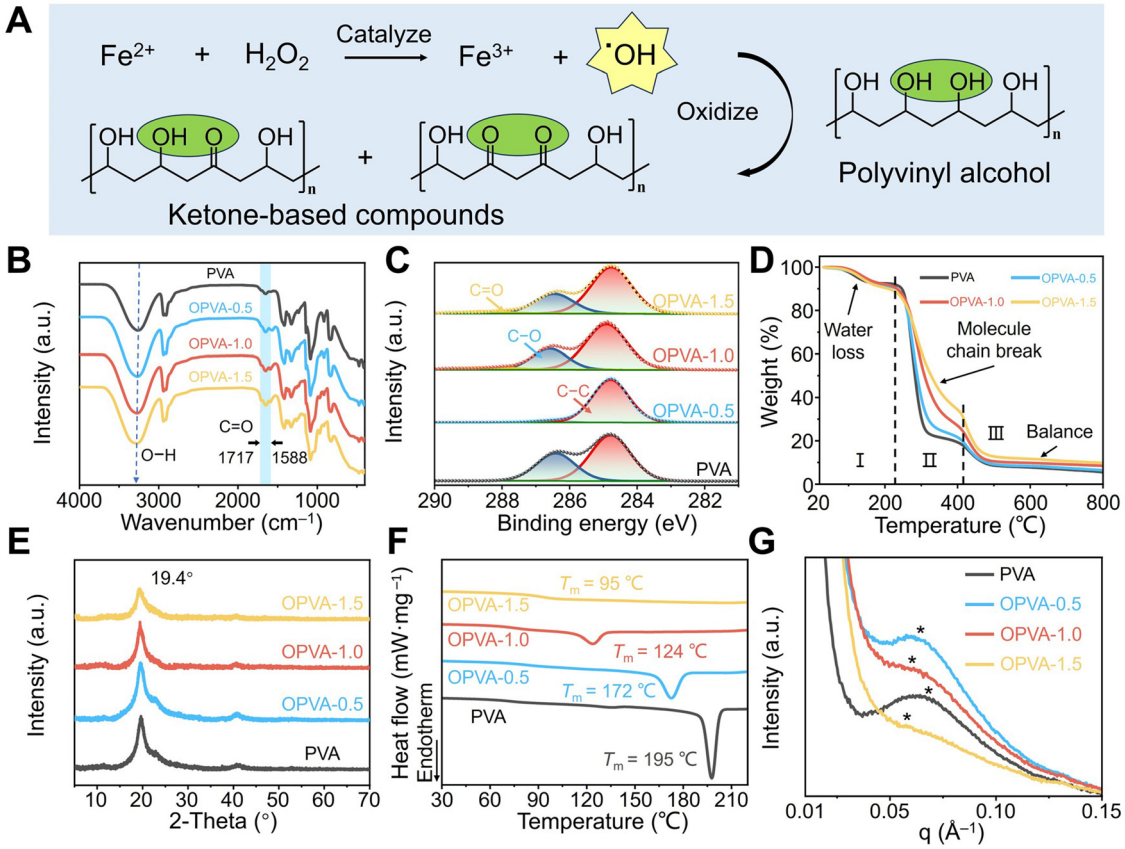

Fig. 1 Structure and crystallization properties of different PVA and OPVA films. (A) Chemical equations for oxidation of PVA by hydrogen peroxide and divalent iron ions. (B) FTIR spectra in the range of 400–4000 cm^{-1}. (C) C1s spectra of the char residues from the different PVA and OPVA samples. (D) TGA curves, (E) XRD patterns, (F) DSC curves, and (G) SAXS profiles of different PVA and OPVA films.

hydroxyl and carboxyl groups on OPVA, and therefore more thermal energy was required to decompose OPVA, leading to an increase in the decomposition temperature.[30] Finally, the weights of the PVA and OPVA samples continuously decreased at 410 °C due to the degradation of the polyene residues, and ultimately the amorphous carbon residues and mineral salt were left behind.[31] The crystallization of macromolecular chains is another crucial indicator of thermal behavior. The X-ray diffraction (XRD) spectra of the PVA, OPVA-0.5, OPVA-1.0, and OPVA-1.5 samples showed a diffraction peak at 2θ = 19.4°, which was assigned to the (101) reflection of the PVA crystals.[32] Compared with pure PVA, the intensity of the diffraction peak obviously decreased in the OPVA sample, indicating that the oxidation of PVA chains significantly suppressed the crystallization behavior of PVA (Fig. 1(E)). Specifically, the formation of a crystalline domain was mainly attributed to hydrogen bonding interactions, which promoted the curling and folding of the PVA molecular chains, and thus accelerated the crystallization phenomenon. However, the consumed hydroxyl groups and the newly produced ketone radicals during the oxidation process weakened the interaction forces between the molecular chains, ultimately leading to a decrease in crystallinity.[33]

In the case of semi-crystalline polymers, the peaks related to the amorphous region in their XRD spectra are generally broad, and therefore crystallinity calculated based on the area integration of the XRD pattern is not sufficiently accurate.[34] Thus, differential scanning calorimetry (DSC) was further employed to verify effect of the PVA oxidation degree on its crystallization behavior. As shown in Fig. 1(F), the melting points of the PVA samples were reduced from the original 195 °C to about 95 °C with an increase in H_2O_2 dosage, and the corresponding intensity of the melting peak was also significantly weakened due to the decrease in crystallinity. Fig. S2 (ESI†) shows that crystallinity of the PVA and OPVA-1.5 samples was 43.9% ± 2.9% and 2.4% ± 0.5%, respectively, confirming that the oxidation process hindered the formation of crystalline domains by weakening the hydrogen bond interactions or relaxing the neat arrangement of molecular chains.[35] Small-angle X-ray scattering (SAXS) was further utilized to determine the average distance between the PVA crystalline domains. As shown in Fig. 1(G), the average distance between the PVA crystalline domains was about 9.78 nm, which was much smaller than that of the OPVA-1.5 sample (~11.85 nm). According to the literature, an increase in the spacing between crystalline regions always indicates a reduction in crystallinity and enhancement in polymer chain flexibility.[36] Benefitting from this relatively wide microstructure sacrificing the crystallization, the macromolecule chains in the OPVA sample had sufficient space for movement, leading to an increase in chain

entanglement. Furthermore, according to the 2D scattering pattern of SAXS (Fig. S3, ESI†), it was evident that the crystallinity of OPVA decreased significantly compared to that of PVA, confirming again that the consumption of the hydroxyl groups by H_2O_2 oxidation reduced the formation of crystalline domains and increased the flexibility of the polymer chains.

3.2. Balance in degradability and mechanical property of OPVA film

Although PVA is a degradable material, its slow degradation rate in natural situations limits its widespread use. Herein, the degradation behaviors of PVA and OPVA were examined by recording their weight changes as a function of time in the soil. As shown in Fig. 2(A) and Fig. S4 (ESI†), there was no significant change in the appearance of PVA and OPVA-0.5 after 28 days of burial in the soil, whereas for the OPVA-1.0 and OPVA-1.5 samples, a certain amount of fragments appeared under the same situations. The further observation of these PVA and OPVA membranes was conducted under a microscope after 7 days of burial in the soil (Fig. 2(B) and Fig. S5, ESI†). All the OPVA specimens exhibited uneven and porous surfaces caused by degradation, and more voids were formed on their surface with an increase in H_2O_2 concentration. In contrast, no obvious morphological changes were observed on the surface of the PVA membrane, expect for the existence of a small amount of sand and gravel. It is worth noting that weight loss of the pure PVA membrane was below 10% after 90 days of burial in the soil, while for the OPVA-1.0 and OPVA-1.5 samples, it reached up to 100% just after 60 and 30 days, respectively (Fig. 2(C)), indicating that the OPVA film achieved nearly complete degradation into H_2O and CO_2 by regulating the degree of oxidation. Moreover, the corresponding weight-average molecular weights

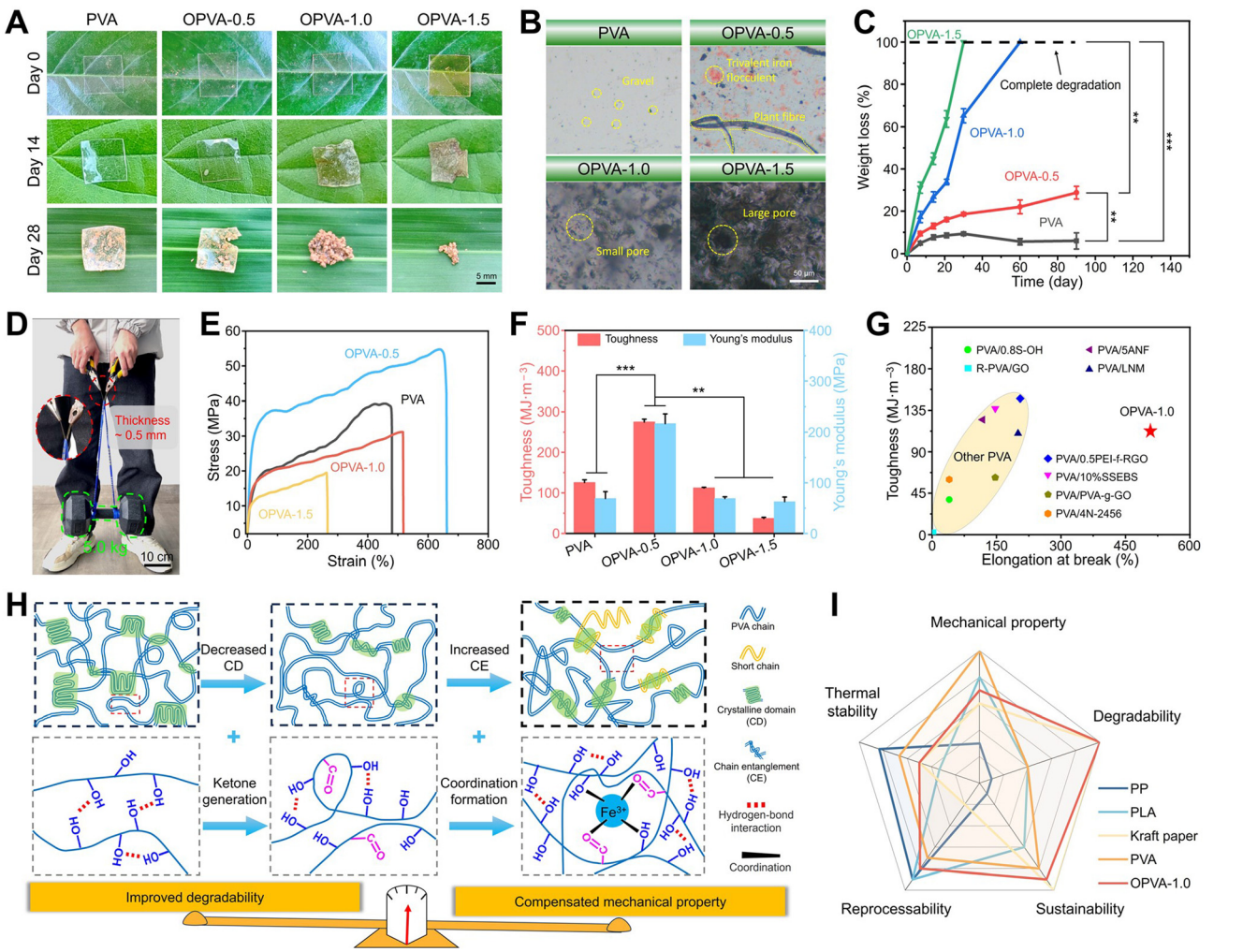

Fig. 2 Degradability and mechanical properties of OPVA film. (A) Digital images of PVA and OPVA buried in the soil. (B) Microscope images of PVA and OPVA buried in the soil for 7 days. (C) Weight loss curves of PVA and OPVA within 90 days. (D) OPVA-1.0 strip with a length of 10 cm, width of 0.5 cm, and thickness of 0.5 mm for carrying dumbbells with a weight of up to 5.0 kg. (E) Stress–strain curves, (F) toughness & Young's modulus, and (G) toughness and elongation at break of OPVA-1.0 film compared with other modified PVA films (name taken from synchronized abbreviations in published articles).[37–44] (H) Mechanism diagram of balance in improved degradation and mechanical compensation of OPVA. (I) Radar chart to compare OPVA-1.0 with commercially available products including PP, PLA, kraft paper, and traditional PVA. All statistical data are represented as mean ± SD (n = 3; $^{**}P < 0.01$, $^{***}P < 0.001$).

of the PVA and OPVA-1.5 samples were 6.42×10^4 and 3.94×10^4 g mol^{-1}, respectively, and this decrease in molecular weight was helpful to accelerate the degradation behavior (Table S1, ESI†).

An improvement in degradation performance is usually at the expense of mechanical properties, and only achieving a balance between degradation behavior and mechanical properties ensures the wide application of materials. Noticeably, the digital image in Fig. 2(D) shows that an OPVA-1.0 strip with a thickness of ~500 μm and width of ~0.5 cm was capable of carrying dumbbells weighing ~5.0 kg without forming any cracks, demonstrating that our fabricated OPVA samples possessed robust load-bearing ability. The mechanical properties of the PVA, OPVA-0.5, OPVA-1.0, and OPVA-1.5 films were quantitatively measured using a texture analyzer (Fig. 2(E)). As shown in Fig. 2(F), the toughness and Young's modulus of the OPVA-0.5 sample were 274.76 ± 7.13 MJ m^{-3} and 216.57 ± 19.17 MPa, which were significantly higher than that of the unoxidized PVA (125.58 ± 6.55 MJ m^{-3} and 68.98 ± 13.47 MPa), respectively. However, all the mechanical performance indicators including tensile strength, Young's modulus, and fracture toughness decreased as the H_2O_2 concentration increased. Under a low H_2O_2 concentration, the iron ions introduced during the oxidation process were coordinated with the hydroxyl groups on the PVA chains, where the combined hydrogen bonding and coordination bonding effects were helpful to reinforce the mechanical properties.[45] However, with a gradual increase in the H_2O_2 concentration, a large number of PVA molecular chains was broken due to the intensification of the oxidation degree, resulting in a conspicuous decrease in molecular weight. In this context, the coordination effect by the iron ions could not compensate for the influence caused by the decline in molecular weight, finally endowing the OPVA-1.5 sample with the relatively lowest mechanical properties among the groups. Based on the systematic evaluation of mechanical properties and degradability, OPVA-1.0 was selected as the main sample for further discussion. As shown in Fig. 2(G), especially for toughness and elongation rate at break, the OPVA-1.0 sample behaved significantly better than other degradable PVA-modified films reported thus far, indicating its great application potential in the field of film packaging.

Significantly, the proposed OPVA film reached a balance in accelerated degradation behavior and robust mechanical performance (Fig. 2(H)). In terms of improved degradability, the difficulty of hydroxyl oxidation is often considered an important reason for the low degradation efficiency of PVA under natural conditions.[46] As displayed in Fig. S6 (ESI†), regardless if PVA oxidase or PVA-DH was employed, its hydroxyl groups should be first oxidized into ketones, and then an aldolase or a diketone hydrolase catalyzes the following enzymatic degradation process.[20,21] Afterwards, the process is repeated until PVA is completely degraded into H_2O and CO_2, which is green and environmentally friendly without the generation of harmful substances. However, both enzymes from specific microorganisms are not universally present in nature. Thus, herein, the hydroxyl groups on the PVA molecular chains were first oxidized into ketone groups by introducing H_2O_2 and Fe^{2+} ion, which are more easily degraded by microbial enzymes. Furthermore, the consumption of some hydroxyl groups during the oxidation process weakened the hydrogen bonds interactions existing between the molecular chains and reduced the crystallinity drastically.[47] It is widely accepted that irregularly organized structures always present poor capability to resist microbial erosion.[48] However, the mechanical properties of the OPVA membrane were not greatly weakened with an improvement in its degradation behavior, but were well-supplemented based on its internal multi-level interactions. After oxidative modification, the entanglement effect of the OPVA molecular chains in the amorphous region was enhanced, and meanwhile some short chains were entangled again with the long chains through hydrogen bonding, resulting in a dense OPVA network to compensate for mechanical loss. In addition, the Fe^{3+} ions existing within the oxidized OPVA film formed dynamic metal coordination bonds with the hydroxyl and ketone groups, further strengthening the internal forces of the OPVA membrane and compensating its mechanical performance by multi-level and multi-dimensional physical interactions.[49]

Furthermore, according to the comparison of the comprehensive properties of our synthesized OPVA-1.0 degradable plastic with some representative commercial products, OPVA-1.0 presented great potential in replacing paper or some traditional plastics due to its thermal stability, recyclability, spontaneous degradation behavior, and sufficient mechanical performance (Fig. 2(I)).[14,50–54] Overall, the oxidation of the hydroxyl groups into ketone compounds was successfully realized by introducing H_2O_2 and Fe^{2+} ions in a facile way, which not only improved the degradation performance of PVA by decreasing its crystalline domains, but also well compensated for its mechanical weakening by the internal multi-level interactions of molecular chain entanglement, hydrogen bonding, and Fe^{3+} ion coordination. This ideal balance between mechanical performance and degradation properties ensures the wide range of applications for the OPVA-1.0 film as a new packaging material in the future.

3.3. Film-formability, washability and self-healing ability of OPVA

Based on the comprehensive consideration of its degradation performance and mechanical property, OPVA-1.0 was selected as the optimal choice to complete the following fruit-preservation experiments. For adapting to different fruits, OPVA-1.0 solutions with different concentrations were prepared for spraying, dipping, and brushing (Fig. 3(A)). Different film-forming methods have specific applications and advantages, which are summarized in Table S2 (ESI†). Furthermore, the processability of the OPVA-1.0 solution as a coating was evaluated by measuring its shear stress or/and viscosity as a function of shear rate. As shown in Fig. 3(B), the solution exhibited representative shear-thinning behavior, where the viscosity of the solution was drastically decreased by nearly three orders of magnitude upon shearing. Movie S1 (ESI†) presents the process of spraying the OPVA-1.0 solution on loquats. Benefitting from the shear-thinning behavior of the OPVA-1.0 solution, a thin and even coating was instantly formed on the surface of the fruits because the high

shear rate at the nozzle reduced the viscosity of the OPVA-1.0 solution but improved its homogeneity.

The advantage of the spraying method is its rapid film formation and ease of use, particularly for coating complex-shaped fruits. To observe the uniformity and thickness of the OPVA membrane formed by spraying onto a banana peel clearly, a fluorescence-labeled reagent of rhodamine B was added into the OPVA-1.0 solution. As shown in Fig. 3(C), the OPVA-1.0 solution formed a thin film on the banana peel and the film could be completely torn off after exerting external

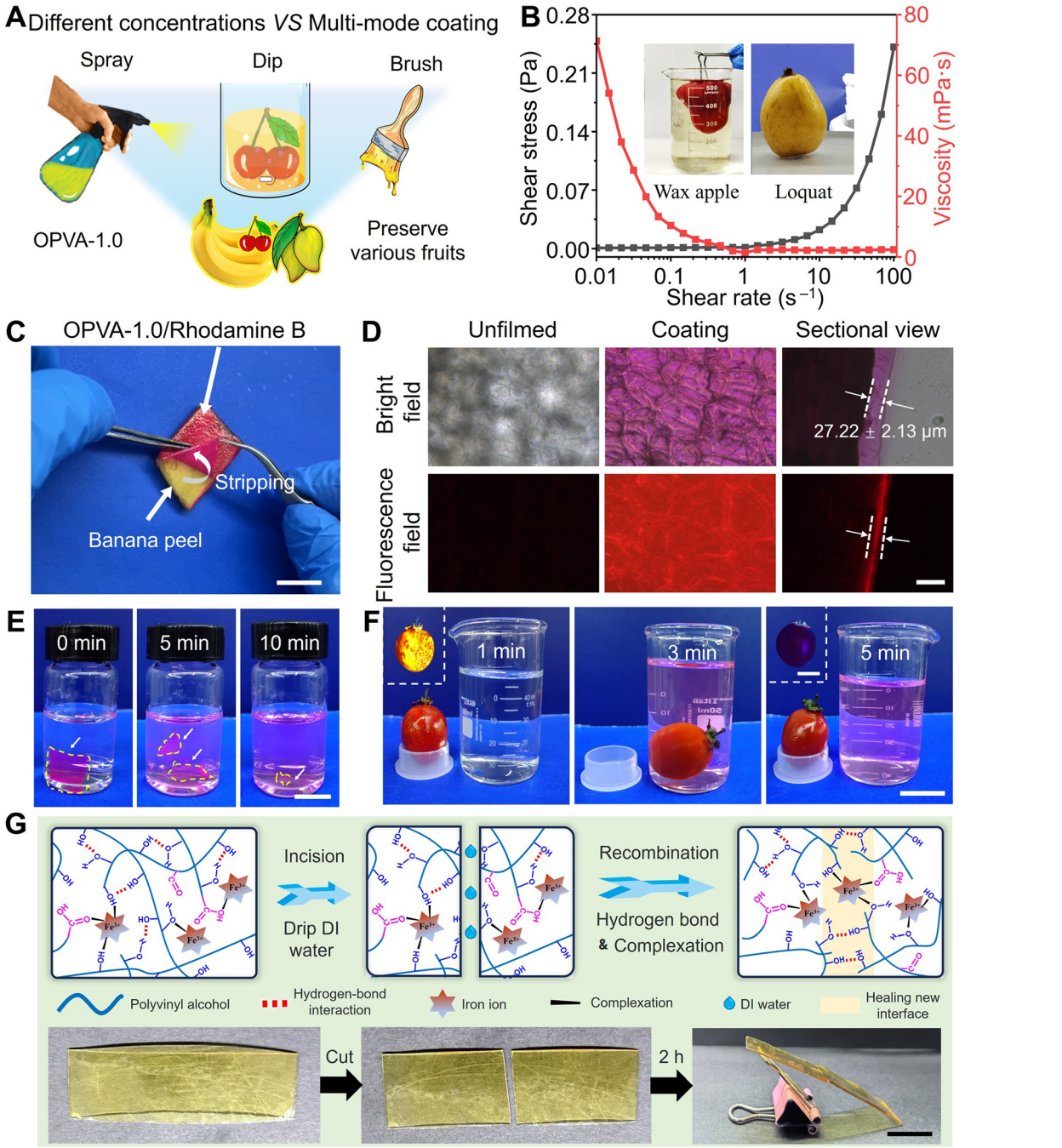

Fig. 3 Film-formability, washability and self-healing ability of OPVA. (A) Schematic diagram of various coating methods. (B) Viscosity and shear stress measurements of OPVA-1.0 coating as a function of shear rate. Insert is a photograph of OPVA-1.0 coated on a loquat and wax apple. (C) Digital image of film formation of OPVA-1.0/rhodamine B mixture on a banana peel (scale bar = 1 cm). (D) Morphology images of banana peel observed under an inverted fluorescence microscope (scale bar = 50 μm). (E) Dissolution process of OPVA-1.0 membrane in deionized water (scale bar = 1 cm). (F) Dissolution process of OPVA-1.0 membrane coated on tomatoes by soaking them in water (scale bar = 2 cm). Inserts are fluorescence images of tomatoes before and after washing under ultraviolet light irradiation (scale bar = 1 cm). (G) Schematic diagram and digital images of self-healing ability of OPVA-1.0 film (scale bar = 1 cm).

force. The surface morphologies of the coated and uncoated banana peels were further observed using an inverted fluorescence microscope. It can be seen in Fig. 3(D) that OPVA-1.0 formed a uniform and transparent film by the spraying method with a thickness of 27.22 ± 2.13 μm; meantime, the structure of the epidermal cells in the surface of the banana peel was clearly observed. To verify the water-washing ability of the OPVA-1.0 membrane coated on fruit surface, a small piece of OPVA-1.0/rhodamine B mixture film with dimensions of 10.0 × 10.0 × 0.2 mm^3 was immersed in deionized water, which completely dissolved after about 10 min (Fig. 3(E)). As shown in Fig. 3(F), the OPVA-1.0/rhodamine B membrane coated on the surface of a tomato was also almost dissolved after placing the tomato in stirring deionized water for 5 min. The inserts in Fig. 3(F) present the prominent variations in fluorescence intensity under UV irradiation, fully demonstrating that the OPVA-1.0 sample not only formed a uniform film on the surface of the fruits quickly, but also possessed the ability to be easily removed upon washing with water without any residue left before consumption.

The film-forming and water-washability of the OPVA-1.0 film are attributed to its dynamically crosslinked hydrogen bonds and coordination interactions, and thus it was natural for us to evaluate its self-healing ability in the presence of water. Collisions during the transportation of fruits result in the formation of cracks, thereby affecting the preservation effect. Thus, the self-healing ability of the film is helpful to establish a new physical barrier for achieving fruit preservation. As shown in Fig. 3(G), two pieces of membrane cut from the original OPVA-1.0 sample were successfully self-healed after being contacted for 2 h with the assistance of deionized water. In detail, the existence of water molecules improved the degree of freedom of the molecular chains in OPVA-1.0 at the interface. Subsequently, benefitting from the entanglement of the molecular chains, reversible hydrogen bonds of the hydroxyl groups, and metal coordination interactions of Fe^{3+}(–OH) or Fe^{3+}(–COOH), eventually a new and intact membrane was formed.[55]

Due to the dynamic reversible nature of hydrogen bonds and metal coordination bonds, the OPVA-1.0 film also allowed convenient welding to be realized with the assistance of water. As shown in Fig. S7A (ESI†), the two OPVA-1.0 films were placed together with an overlapping area of 1.0 × 1.0 cm^2, and then 10.0 μL of deionized water was dropped onto the overlapping portion. After pressing the two films for 1 min, a monolithic OPVA strip was instantly formed through the welding effect. This quick, facile, and satisfactory welding ability guaranteed the fabrication of various products using the OPVA-1.0 films. As illustrated in Fig. S7B (ESI†), packaging bags and zip-lock bags were easily prepared by completing the three steps of bending, folding, and water welding. Moreover, our prepared handbags were utilized for lifting different items with a weight in the range of 0–200 g and holding beans (Fig. S7C, ESI†). It was obvious that the beans did not fall apart as the water-welded interface was facing down, further indicating a good sealing performance and interfacial-connection strength. As shown in Fig. S7D (ESI†), a comparison of the mechanical properties between various water-welded OPVA strips and the pristine films was conducted through tensile tests. There was no noticeable change in the tensile strength and Young's modulus before and after welding, but a significant reduction in elongation at break was presented, which was ascribed to the existence of some inevitable defects at the interfaces impairing the ability to resist rupture.[56] Nevertheless, the lowest strain value was still above 140%, meeting the daily-use requirements of packaging materials. As a type of supramolecular film dynamically crosslinked by hydrogen bonds and coordination interactions, it was natural for us to evaluate its reusability in the presence of water. As shown in Fig. S8 (ESI†), the recycled OPVA film also presented comparable mechanical properties after ten cycles of operation. The tensile strength and Young's modulus of the OPVA-1.0 sample in the 10th cycle were 27.21 ± 1.38 and 61.90 ± 4.74 MPa, which were comparable to the level in the original state (31.11 ± 1.60 and 68.97 ± 3.44 MPa), respectively. Typically, degradable PVA modified by chemical methods has weakened mechanical properties due to the destruction of its molecular structure, intermolecular force, and crystallization, thus limiting its widespread applications.[57] In this study, the constructed OPVA-1.0 not only had the ability to degrade in natural soil within 60 days, but also maintained good mechanical properties after 10 cycles of recycling process.

3.4. Fruits freshness preservation ability of OPVA film

The complex rotting process of fresh fruits primarily includes dehydration, transition from respiratory to fermentative metabolism, microbial growth, and senescence.[58] A gaseous environment composed of H_2O, CO_2, and O_2 directly affects the physiological metabolism of fruits and development of food spoilage.[59] Specially, rapid aerobic and anaerobic respiration after fruits picking will cause fruits to age and decay, respectively. Consequently, an ideal atmosphere should restrain the physiological metabolism of fruits to a low degree, and meanwhile inhibit the proliferation of microorganisms, contributing to the preservation of fresh fruits.[60] In this case, PVA containing a large number of hydroxyl groups is considered an ideal oxygen-barrier material, which generally presents an extremely-low O_2 passage rate due to its polar surface.[61] In the as-fabricated OPVA-1.0 film, its molecular polarity obviously decreased given that a portion of the hydroxyl groups in the original PVA was consumed during the oxidation process, finally resulting in an increase of the O_2 passage rate to prevent the anaerobic respiration of fruits. In addition, a dense and uniform membrane will completely intercept the CO_2 generated by the respiration of fruits, thus further enhancing the anaerobic respiration of fruits in a hypoxic environment, which results in their accelerated decay.[62] Fortunately, the formation of ketone groups in the OPVA-1.0 molecular chains endowed the film with an improved attraction to CO_2, and subsequently helped to discharge a small amount of CO_2 into the air. Moreover, the hydrophilic OPVA was prone to absorb moisture produced by the respiration of the fruits or directly from the air due to the presence of hydrophilic groups and the hydrogen bonding effect with water molecules. The formation of a water-retaining layer is extremely important for

maintaining the freshness of fruits.[63] Compared with the PVA membrane, an atmosphere composed of a higher O_2 content, a lower CO_2 concentration, and a higher H_2O content could be generated between the OPVA-1.0 film and the fruits, finally slowing down their anaerobic respiration and inhibiting their decay (Fig. 4(A)).

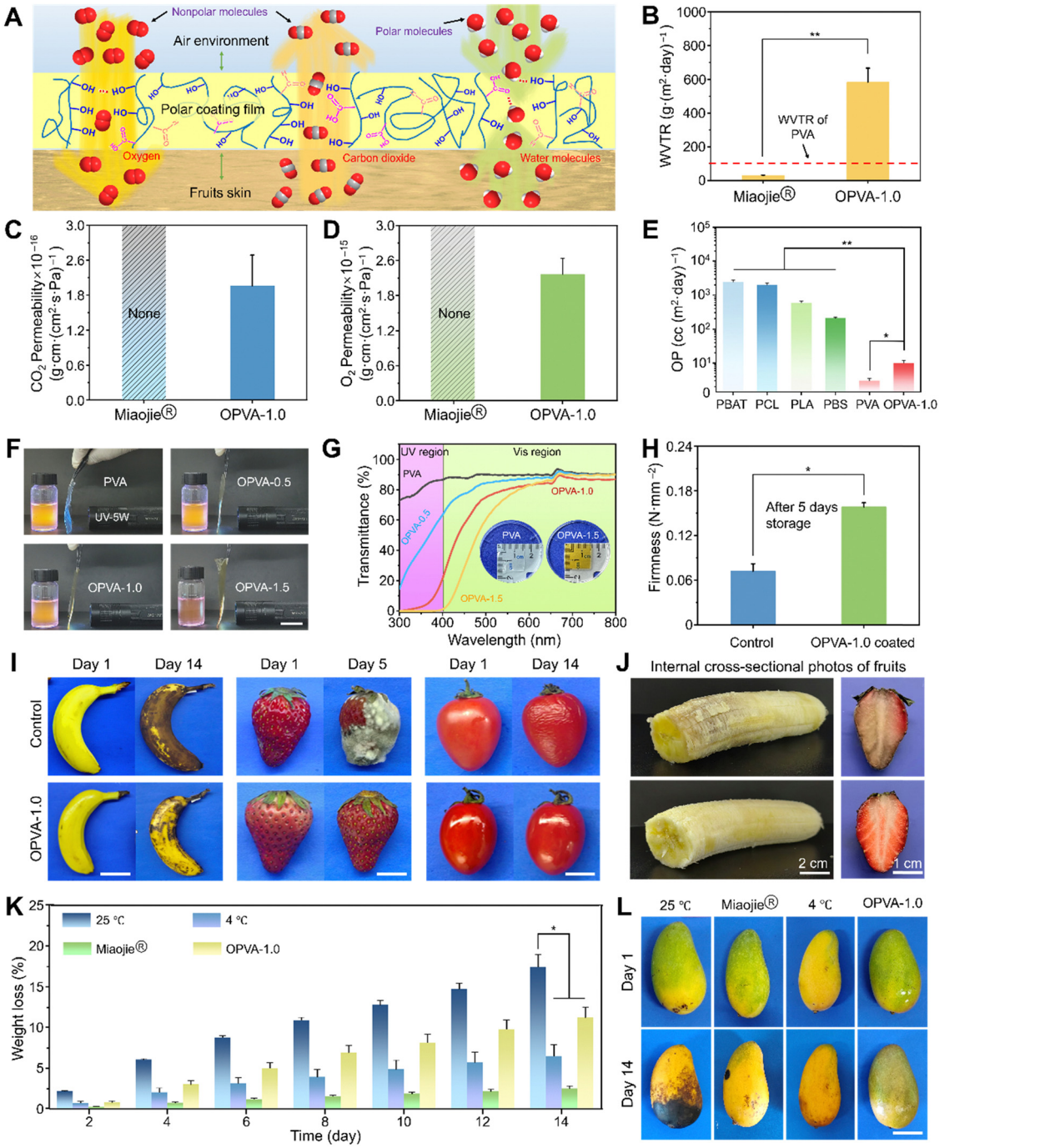

Fig. 4 Effect and mechanism of OPVA-1.0 coating on fruit ripeness. (A) Schematic diagram of fruit preservation mechanism of OPVA-1.0 film. (B) WVTR of OPVA-1.0 films compared to commercial Miaojie® cling film. (C) CO_2 permeability of OPVA-1.0 films compared to commercial Miaojie® cling film. (D) O_2 permeability of OPVA-1.0 films compared to commercial Miaojie® cling film. (E) O_2 permeance (OP) of OPVA-1.0 films compared to other commonly used coating materials. (F) Digital images of placing PVA or OPVA film between rhodamine B solution and UV lamp (scale bar = 2 cm). (G) UV-vis transmittance curves of PVA and OPVA. (H) Firmness of bare and coated strawberries after storage for different times. (I) Time-lapse photographs of bare and coated fruits (banana: scale bar = 5 cm; strawberry and tomato: scale bar = 1 cm). (J) Cross-sectional photos of fruits showing their interior quality. (K) Weight loss of mangoes as a function of time under four situations. (L) Time-lapse photographs of mangoes kept in four different environments for 14 days: room temperature (25 °C), refrigeration (4 °C), commercial Miaojie® cling film, and OPVA-1.0 coating (scale bar = 5 cm). All statistical data are represented as mean ± SD (n = 3; *P < 0.05, **P < 0.01).

To verify whether the OPVA sample has promising potential to preserve the freshness of fruits, the permeability of H_2O, CO_2, and O_2 in the OPVA-1.0 film was compared with that of the commercial Miaojie® cling film. As shown in Fig. 4(B), the water vapor transmission rate (WVTR) of the OPVA film was as high as 583.5 ± 82.4 g $(m^2\ day)^{-1}$, which was significantly higher than that of the commercial Miaojie® cling film (29.3 ± 2.4 g $(m^2\ day)^{-1}$) and pure PVA material ($\sim 10^2$ g $(m^2\ day)^{-1}$).[64] Notably, a high moisture level is often needed during the storage of fresh fruits, while an exorbitant moisture level will result in food spoilage. The upper limit of WVTR suitable for fruit preservation is determined as 10^3 g $(m^2\ day)^{-1}$.[64] Therefore, the OPVA-1.0 film prepared in the current study not only transported the water vapor generated by the respiration of fruits to avoid microbial reproduction, but also adjusted the moisture content within a reasonable range to maintain the freshness of the fruits. The permeabilities of CO_2 and O_2 through the OPVA-1.0 film were $(1.96 \pm 0.53) \times 10^{-16}$ g cm $(cm^2\ s\ Pa)^{-1}$ and $(2.16 \pm 0.28) \times 10^{-15}$ g cm $(cm^2\ s\ Pa)^{-1}$, respectively. However, no data was measured in the Miaojie® cling film group because it was too dense to permeate CO_2 and O_2 (Fig. 4(C) and (D), respectively). The OPVA-1.0 solution formed a protective film on the surface of the fruits instantly through spraying, which successfully realized the aerobic respiration of the fruits by promoting the outflow of CO_2 and the inflow of O_2. Compared to commercial plastic wraps, the OPVA-1.0 coating possessed better gas-regulation ability, showing great possibility for inhibiting the decay process of fruits and extending their shelf life.

The O_2 permeance rates of other degradable materials (PBAT, PCL, PLA, and PBS) were summarized for comparison with the OPVA-1.0 membrane.[65] As shown in Fig. 4(E), an oxygen permeability (OP) value of over 10^2 cc $(m^2\ day)^{-1}$ was exhibited by the other materials, which is obviously higher than that in the PVA and OPVA-1.0 samples. Noticeably, the traditional plastic wraps acting as a barrier to O_2 are prone to inducing the occurrence of anaerobic respiration in fruits, resulting in the appearance of deterioration in the fruits after the O_2 is depleted.[66] In contrast, an excessively high O_2 permeance also cannot maintain the freshness of fruits because an important parameter of fruit ripening is relevant to oxidation.[67] Overall, OPVA-1.0 with moderate permeability towards H_2O, CO_2, and O_2 will become a competitive eco-friendly material in the future due to its degradability and fruit preservation performance.

Notably, intense UV irradiation easily leads to changes in product properties and causes some irreparable damage, especially in certain UV-sensitive products (*e.g.*, food and pharmaceuticals).[68] Therefore, the UV absorption ability of packaging materials is particularly important for fruit preservation. As shown in Fig. 4(F), the fluorescence intensity of the rhodamine B solution was high when the PVA film was placed between the solution and UV lamp. Alternatively, the fluorescence intensity of the rhodamine B decreased significantly with an increase the oxidation degree of OPVA, especially for the OPVA-1.5 group, where only subtle UV light passed through the film, indicating that OPVA has a very strong absorption effect towards UV light. Furthermore, the degree of transmittance of the PVA and OPVA samples was determined using a visible ultraviolet spectrophotometer to further verify their UV absorption ability quantitatively. As revealed in Fig. 4(G), there was no obvious difference in membrane transmittance before and after the modification in the wavelength range of 600–800 nm. In contrast, the pure PVA and OPVA samples presented different absorption capabilities at a wavelength lower than 400 nm. Particularly for the OPVA-1.5 group, it achieved almost 100% absorption towards ultraviolet light, which is probably owing to the formation of carbonyl groups in the OPVA molecular chains. Conventional ultraviolet absorption strategies rely on the addition of substances containing π–π stacking groups or color-generating groups such as carbon dots, tannins, and protocatechualdehyde, which unfortunately create new issues of declining transparency, uneven dispersion, and biotoxicity.[69] Herein, the facile oxidation treatment of PVA endowed the OPVA product with an improved ability of blocking ultraviolet, laying a theoretical foundation for its application in the field of fruit preservation.

In the current study, we evaluated the effectiveness of the OPVA-1.0 coating in preserving the freshness of fruits by employing some readily available and representative fruits, such as bananas, strawberries, tomatoes, and mangoes. At 5 or 14 days post-purchase, the uncoated fruits all showed enzymatic browning, decaying with white mold, or dehydration shrinkage, whereas the coated fruits still retained a relatively good appearance or freshness even after two weeks (Fig. 4(I) and Movies S2, S3, ESI†). By regularly measuring the weight changes in the bananas, strawberries, and tomatoes, a huge difference was observed in terms of weight loss between the coated- and bare-fruits (Fig. S9, ESI†). Especially in the case of the bare strawberries, the weight loss rate reached up to 60%, which almost twice that as the OPVA-1.0 film group. For assessing the effect of the OPVA film on the fruit quality after prolonged exposure, the interior property variations of bananas and strawberries were further observed. As shown in Fig. 4(J), the fruits in the control group were rotting and lost their original color. In contrast, the OPVA-coated fruits still retained their normal color and sufficient moisture, indicating that our synthesized OPVA-1.0 material did not have any negative impact on the fruit quality and the diffusion of Fe^{3+} with an extremely low concentration could be ignored. Firmness is an important indicator to evaluate the freshness of fruits, where the softening of fruits is usually accompanied by the loss of water, degradation of cellulose, and reduction in pectin content.[70] For further quantitative evaluation, firmness tests were conducted on the coated and uncoated strawberries after 5 days of storage. As shown in Fig. 4(H), the firmness of the coated and bare strawberries was 0.15 and 0.07 N mm^{-2}, respectively, indicating that our fabricated OPVA-1.0 film possessed the ideal water retention capability and freshness preservation ability towards perishable fruits.

To compare the fruit preservation efficacy between our newly synthesized OPVA-1.0 coating and other currently established

strategies, mangoes were further selected for the subsequent experiments. They were divided into four groups, including uncoated, packaged using commercial Miaojie® cling film, placed in a refrigerator at 4 °C to simulate cold chain transportation, and sprayed with the OPVA-1.0 solution. As shown in Fig. 4(L) and Movie S4 (ESI†), after keeping the untreated mangoes at room temperature for 14 days, they showed a large number of spots and were no longer edible. Slightly better, in the commercial cling film group, there were some small black spots on the mangoes. The mangoes placed in the refrigerator or coated with the OPVA-1.0 film presented the best appearance, especially the mangoes in the OPVA-1.0 group, where the lowest level of maturity and the highest degree of freshness were observed. Weight monitoring of the mangoes was also conducted for these four groups, and it was found that storage strategy dependent on Miaojie® cling film presented the best water retention effect (Fig. 4(K)). Although the OPVA-1.0 film did not show the highest water retention rate, the greenest color of the mangoes after 14 days indicated its good ability to inhibit mango ripening. Consequently, a combination of the OPVA film with refrigeration will be helpful to achieve ideal fruit preservation for long-distance transportation and cross-regional sales.

3.5. Biocompatibility *in vitro* and biosafety *in vivo* of OPVA

Although the OPVA-1.0 film possessed good water-washability, it was still difficult to guarantee that was no residue left on the fruit surface. To understand the effect of OPVA residue on the organisms as it was ingested without thorough cleaning, it was necessary to assess its biocompatibility *in vitro* and biosafety *in vivo*. For the *in vitro* biocompatibility test, a mouse embryonic fibroblast cell line (NIH/3T3) was employed to be co-cultured with extracts of the PVA, OPVA-0.5, OPVA-1.0 and OPVA-1.5 films for 1, 3, and 5 days. Firstly, the strong green signals, as revealed in Fig. 5(A), suggested that the NIH/3T3

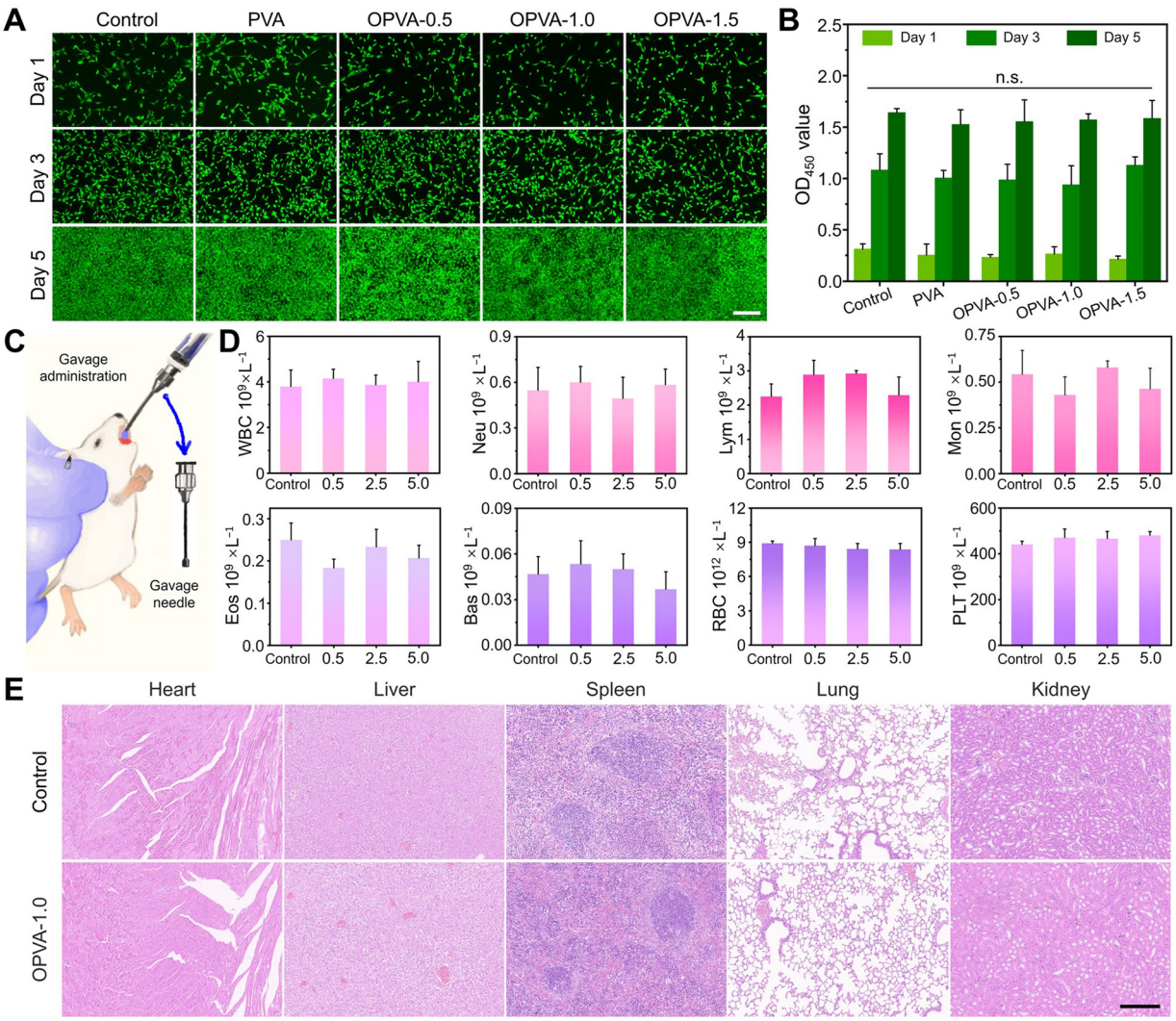

Fig. 5 *In vitro* biocompatibility and *in vivo* biosafety of OPVA. (A) Live/dead staining images (scale bar = 200 μm) and (B) CCK-8 assay result of NIH/3T3 cells after being *co*-cultured with OPVA for 1, 3, and 5 days. (C) Schematic diagram of mouse gavage. (D) Blood biochemical parameters of mice in the control and experimental groups. (E) Representative H&E staining images of visceral organs in the control and experimental mice (scale bar = 200 μm). All statistical data are represented as mean ± SD (n = 3, n.s.: not significance).

cells possessed a good proliferation rate after 5 days incubation in the presence of OPVA. Moreover, the cell counting kit-8 (CCK-8) assay was further performed and a similar result was observed (as shown in Fig. 5(B)). After being co-cultured with the NIH/3T3 cells for 1, 3, and 5 days, the optical density (OD) values of the OPVA film-treated groups were not significantly different from that of the control group, further confirming that our-fabricated OPVA sample has ideal biocompatibility.

To evaluate the *in vivo* biosafety of our synthesized OPVA, a daily quantitative gavage containing OPVA aqueous solutions in different concentrations of 0.5, 2.5, and 5.0 mg mL^{-1} was administered to the mice for 21 consecutive days, while drinking water was regarded as the control group (Fig. 5(C)). During the whole experimental period, the weight changes in the mice were monitored in real time. Afterwards, serum samples and the visceral organs (including heart, liver, spleen, lung, and kidney) of all the mice were collected for biological and histological analyses to verify whether the OPVA-1.0 residue was enriched in the blood or organs of the mice, and thereby negatively affected their health. Noticeably, there was no obvious difference in crucial blood biochemical parameters between the experimental and control groups (Fig. 5(D)), such as white blood cells (WBC), neutrophil granulocytes (Neu), lymphocytes (Lym), monocytes (Mon), eosinophilic granulocytes (Eos), basophilic granulocytes (Bas), red blood cells (RBC), and thrombocytes (PLT).

Furthermore, tissue sections of the visceral organs in the experimental and control groups were subjected to hematoxylin and eosin (H&E) staining for histological examination. As shown in Fig. 5(E), compared with the mice in the control group, no lipid droplets, inflammatory reactions, or fibrosis were observed in the histological images of the experimental mice, indicating that the OPVA-1.0 sample did not exhibit any biological toxicity and its residue did not influence the healthy conditions of the organs through Fe^{3+} migration. Regarding the body weight variations in the mice after gavage, there was also no obvious difference between the two groups (Fig. S10, ESI†). Notable, PVA is distinguished among the diverse polymer materials due to its ideal biocompatibility and biological non-toxicity and it is approved by the U.S. Food and Drug Administration (FDA) for application in packaging meat and poultry products.[71] Herein, our proposed oxidation-modification strategy relying on H_2O_2 and Fe^{2+} did not introduce any organic solvents, and the oxidation products did not contain any toxic chemical structures such as benzene and its derivatives. Also, despite the inevitable introduction of Fe^{3+}, its concentration in the OPVA-1.0 solution was as low as 100 μg L^{-1}, meeting the requirements for a safe iron content in food-packaging materials.[71] Overall, both the *in vitro* biocompatibility and *in vivo* biosafety results amply demonstrated that our proposed OPVA-1.0 was completely non-toxic, which will not remain in the bloodstream or migrate to biological organs when applied as a packaging material in the field of fruit preservation.

4. Conclusions

In the current study, we proposed an OPVA membrane with improved degradability, sufficient mechanical performance, and prolonged fruit preservation behavior, which was obtained by a facile and environment-friendly modification strategy. Specifically, $^{\bullet}OH$ produced by the reaction between H_2O_2 and iron ions led to the formation of ketone groups and a decrease in crystalline domains, enabling the ideal degradation performance of OPVA-1.0 after being buried in natural soil for ~60 days. Alternatively, this improved degradation rate was not acquired at the expense of mechanical properties, and our proposed OPVA film achieved a balance between accelerated degradation behavior and robust mechanical performance, which was dependent on the multi-level interactions of molecular chains entanglement, hydrogen bonding, and Fe^{3+} ion coordination. More interestingly, the rheological testing, cell viability *in vitro*, and biosafety *in vivo* results further confirmed that the OPVA-1.0 film possessed spray film-forming ability, recyclability, and biocompatibility, laying a solid foundation for its wide application for fruit preservation. As a potential preservative film, OPVA-1.0 extended the shelf life of various fruits to 5–14 days, which was comparable to or even better than that of the commercial Miaojie® cling film. Overall, this work not only solved the problem of difficult degradation of PVA materials in the natural environment, but also presented a new understanding of PVA as a functional coating for fruit preservation.

In comparison with other widely used products such as traditional fruit waxing, the advantages of the OPVA film are mainly reflected in the following three aspects. Firstly, the OPVA sample offers multiple usage methods including spray coating, dip coating, and brush coating; meanwhile, its water-washability ensures its convenient removal from fruits during the routine cleaning process. Secondly, it has good UV absorption ability, significantly reducing the damage of fruits by UV light. Finally, OPVA demonstrated excellent biocompatibility and biosafety, unlike traditional fruit waxing with the potential risk of accumulated toxicity of trace elements. However, there are still some limitations in the exploration of the practical application scenario of the OPVA film and more in-depth studies related to its features are necessary for its comprehensive demonstration. For example, OPVA is difficult to be evenly coated onto some hairy fruits or waxed fruits because their fluffy or hydrophobic surface always inhibits the OPVA film-forming process, and finally has a negative impact on its fruit preservation performance. In addition, the good water-washability of the OPVA film indicates that it cannot be applied in an aquatic environment due to its uncontrollable underwater stability. Therefore, achieving a balance between water-resistance ability and water-washability of the OPVA coating is the focus of our future research, which will help further expand the application scenarios of OPVA beyond fruit preservation. Finally, there is no sufficient discussion in the current study about all the possible problems that might arise during the OPVA industrialization process. In the near future, we will find a substitute factory as a pilot for adjusting its processing technology and realizing sample batch production.

Author contributions

Yi Lu: conceptualization, data curation, formal analysis, investigation, writing – original draft. Guoming Liu:

conceptualization, data curation, formal analysis, writing – review. Kaixin Zhang: investigation, methodology, visualization. Ziyi Wang: investigation, methodology, resources. Peijie Xiao: investigation, methodology. Changhua Liu: investigation, methodology. Longying Deng: investigation, methodology. Fenglu Li: methodology. Gaoxing Pan: visualization. Shuxian He: methodology. Jiefeng Gao: conceptualization, writing – review. Jin Zhang: conceptualization, funding acquisition, resources, supervision, writing – review & editing.

Data availability

The data supporting this article have been included as part of the ESI.†

Conflicts of interest

The authors declare no conflict of interest.

Acknowledgements

This work was financially supported by the National Key R&D Program of China (grant no. 2022YFB3808000), the National Natural Science Foundation of China (grant no. U23A20490), and the Project for High-Level Talent Innovation and Entrepreneurship of Quanzhou (grant no. 2022C016R). The authors also gratefully acknowledged the kindly financial support provided by the Top Young Talents of Foal Eagle Program of Fujian Province to Jin Zhang. Thanks to the Fujian College Association Instrumental Analysis Center of Fuzhou University for providing testing support.

References

1 S. Jung, Y. Cui, M. Barnes, C. Satam, S. Zhang, R. A. Chowdhury, A. Adumbumkulath, O. Sahin, C. Miller, S. M. Sajadi, L. M. Sassi, Y. Ji, M. R. Bennett, M. Yu, J. Friguglietti, F. A. Merchant, R. Verduzco, S. Roy, R. Vajtai, J. C. Meredith, J. P. Youngblood, N. Koratkar, M. M. Rahman and P. M. Ajayan, *Adv. Mater.*, 2020, **32**, e1908291.
2 G. Schmidt-Traub, M. Obersteiner and A. Mosnier, *Nature*, 2019, **569**, 181–183.
3 C. Zhou, J. Bai, F. Zhang, R. Zhang, X. Zhang, K. Zhong and B. Yan, *Carbohydr. Polym.*, 2023, **321**, 121293.
4 Q. Hu, F. Zhou, N. K. Ly, J. Ordyna, T. Peterson, Z. Fan and S. Wang, *ACS Nano*, 2023, **17**, 8586–8597.
5 X. Sun, J. Wang, M. Dong, H. Zhang, L. Li and L. Wang, *Trends Food Sci. Technol.*, 2022, **119**, 122–132.
6 Y. Li, S. Li and J. Sun, *Adv. Mater.*, 2021, **33**, e2007371.
7 Y. Yang, L. Zhang, J. Zhang, Y. Ren, H. Huo, X. Zhang, K. Huang and Z. Zhang, *ACS Appl. Mater. Interfaces*, 2023, **15**, 4505–4515.
8 M. Grosjean, L. Gangolphe and B. Nottelet, *Adv. Funct. Mater.*, 2023, **33**, 2205315.
9 N. E. Kochkina and N. D. Lukin, *Int. J. Biol. Macromol.*, 2020, **157**, 377–384.
10 Z. M. Han, D. H. Li, H. B. Yang, Y. X. Zhao, C. H. Yin, K. P. Yang, H. C. Liu, W. B. Sun, Z. C. Ling, Q. F. Guan and S. H. Yu, *Adv. Funct. Mater.*, 2022, **32**, 2202221.
11 C. Liu, P. Luan, Q. Li, Z. Cheng, X. Sun, D. Cao and H. Zhu, *Matter*, 2020, **3**, 2066–2079.
12 Y. Yu, Z. Guo, Y. Zhao, K. Kong, H. Pan, X. Xu, R. Tang and Z. Liu, *Adv. Mater.*, 2022, **34**, 2107523.
13 X. Fang, N. Tian, W. Hu, Y. Qing, H. Wang, X. Gao, Y. Qin and J. Sun, *Adv. Funct. Mater.*, 2022, **32**, 2208623.
14 G. Zhou, H. Zhang, Z. Su, X. Zhang, H. Zhou, L. Yu, C. Chen and X. Wang, *Adv. Mater.*, 2023, **35**, e2301398.
15 T. Li, X. Li, J. Yang, H. Sun and J. Sun, *Adv. Mater.*, 2023, **35**, 2307990.
16 C. Chen, W. Sun, J. Wang and D. J. Gardner, *Carbohydr. Polym.*, 2023, **321**, 121315.
17 X. Zhao, Z. Han, S. Zhang, G. Abuduaini, X. Wen, T. Liu and Z. Cheng, *Food Packag. Shelf Life*, 2023, **40**, 101163.
18 Q. Pan, C. Zhou, Z. Yang, Z. He, C. Wang, Y. Liu, S. Song, H. Gu, K. Hong, L. Yu, Y. Qu and P. Li, *Food Chem.*, 2022, **387**, 132878.
19 Y.-P. Lin, R. Dhib and M. Mehrvar, *J. Environ.*, 2021, **8**, 116.
20 H. Bian, M. Cao, H. Wen, Z. Tan, S. Jia and J. Cui, *Int. J. Biol. Macromol.*, 2019, **124**, 10–16.
21 G. von Haugwitz, K. Donnelly, M. Di Filippo, D. Breite, M. Phippard, A. Schulze, R. Wei, M. Baumann and U. T. Bornscheuer, *Angew. Chem., Int. Ed.*, 2023, **62**, 202216962.
22 M. I. Voronova, O. V. Surov, S. S. Guseinov, V. P. Barannikov and A. G. Zakharov, *Carbohydr. Polym.*, 2015, **130**, 440–447.
23 J. Zeng, F. Bian, J. Wang, X. Li, Y. Wang, F. Tian and P. Zhou, *J. Synchrotron Radiat.*, 2017, **24**, 509–520.
24 R. Zhang, Q. Zhang, Y. Ji, F. Su, L. Meng, Z. Qi, Y. Lin, X. Li, X. Chen, F. Lv and L. Li, *Soft Matter*, 2018, **14**, 2535–2546.
25 H. Zhou, H. Zhang, Y. He, B. Huang, C. Zhou, G. Yao and B. Lai, *Appl. Catal., B*, 2021, **286**, 119900.
26 L. Čamdžić and E. E. Stache, *J. Am. Chem. Soc.*, 2023, **145**, 20311–20318.
27 K. Zhang, Q. Guo, Y. Wang, P. Cao, J. Zhang, M. Heggen, J. Mayer, R. E. Dunin-Borkowski and F. Wang, *ACS Catal.*, 2023, **13**, 3164–3169.
28 Y. Wang, Y. Xie, X. Xie, D. Wu, H. Wu, X. Luo, Q. Wu, L. Zhao and J. Wu, *Adv. Funct. Mater.*, 2023, **33**, 2210224.
29 Y. F. Jiang, X. F. Qin, F. Zhu, Y. F. Zhang, X. C. Zhang, W. Hartley and S. G. Xue, *Chem. Eng. J.*, 2023, **451**, 139008.
30 S. S. Channe, R. Singh and S. G. Kulkarni, *Polym. Bull.*, 2024, **81**, 3403–3438.
31 P. S. Thomas, J. P. Guerbois, G. F. Russell and B. J. Briscoe, *J. Therm. Anal. Calorim.*, 2001, **64**, 501–508.
32 F. Yang, J. Li, Y. Long, Z. Y. Zhang, L. F. Wang, J. J. Sui, Y. T. Dong, Y. Z. Wang, R. Taylor, D. L. Ni, W. B. Cai, P. Wang, T. Hacker and X. D. Wang, *Science*, 2021, **373**, 337.
33 L. Liu, M. Zhu, X. Xu, X. Li, Z. Ma, Z. Jiang, A. Pich, H. Wang and P. Song, *Adv. Mater.*, 2021, **33**, 2105829.
34 K. S. Salem, N. K. Kasera, M. A. Rahman, H. Jameel, Y. Habibi, S. J. Eichhorn, A. D. French, L. Pal and L. A. Lucia, *Chem. Soc. Rev.*, 2023, **52**, 6417–6446.

35 X. Hou, B. Huang, L. Zhou, S. Liu, J. Kong and C. He, *Adv. Mater.*, 2023, **35**, 2301532.
36 M. Zhang, Y. Yang, M. Li, Q. Shang, R. Xie, J. Yu, K. Shen, Y. Zhang and Y. Cheng, *Adv. Mater.*, 2023, **35**, 2301551.
37 L. Liu, A. H. Barber, S. Nuriel and H. D. Wagner, *Adv. Funct. Mater.*, 2005, **15**, 975–980.
38 H. K. Cheng, N. G. Sahoo, Y. P. Tan, Y. Pan, H. Bao, L. Li, S. H. Chan and J. Zhao, *ACS Appl. Mater. Interfaces*, 2012, **4**, 2387–2394.
39 Y. Q. Li, T. Yu, T. Y. Yang, L. X. Zheng and K. Liao, *Adv. Mater.*, 2012, **24**, 3426–3431.
40 P. Song, Z. Xu, Y. Lu and Q. Guo, *Macromolecules*, 2015, **48**, 3957–3964.
41 L. Shao, J. Li, Y. Guang, Y. Zhang, H. Zhang, X. Che and Y. Wang, *Mater. Des.*, 2016, **99**, 235–242.
42 Y. Guan, W. Li, Y. Zhang, Z. Shi, J. Tan, F. Wang and Y. Wang, *Compos. Sci. Technol.*, 2017, **144**, 193–201.
43 P. Song and H. Wang, *Adv. Mater.*, 2020, **32**, e1901244.
44 X. Zhang, W. Liu, W. Liu and X. Qiu, *Int. J. Biol. Macromol.*, 2020, **142**, 551–558.
45 Z. Zhou, T. Liu, W. Zhou, H. Chen, Y. Bian, S. Gong, S. Q. Shi and J. Li, *Composites, Part B*, 2022, **247**, 110349.
46 Y. Wang, H. Wang, H. Jin, X. Zhou and H. Chen, *J. Environ. Manage.*, 2022, **304**, 114305.
47 D. H. Li, Z. M. Han, Q. He, K. P. Yang, W. B. Sun, H. C. Liu, Y. X. Zhao, Z. X. Liu, C. N. Y. Zong, H. B. Yang, Q. F. Guan and S. H. Yu, *Adv. Mater.*, 2022, **35**, 2208098.
48 H. Kwak, H. Kim, S. A. Park, M. Lee, M. Jang, S. B. Park, S. Y. Hwang, H. J. Kim, H. Jeon, J. M. Koo, J. Park and D. X. Oh, *Adv. Sci.*, 2022, **10**, 2205554.
49 Y. Lyu, R. Guo, Z. Lin, F. Zhai, T. Wu, P. Jiang, Z. Ji, S. Ma, X. Shi and X. Wang, *Adv. Funct. Mater.*, 2023, **33**, 2306300.
50 W. Chen, P. Zhang, R. Zang, J. Fan, S. Wang, B. Wang and J. Meng, *Adv. Mater.*, 2020, **32**, e1907413.
51 Y. Ma, J. Stubb, I. Kontro, K. Nieminen, M. Hummel and H. Sixta, *Carbohydr. Polym.*, 2018, **179**, 145–151.
52 D. G. Papageorgiou, I. A. Kinloch and R. J. Young, *Compos. Sci. Technol.*, 2016, **137**, 44–51.
53 D. Stoof and K. Pickering, *Composites, Part B*, 2018, **135**, 110–118.
54 X. Wang, Z. Pang, C. Chen, Q. Xia, Y. Zhou, S. Jing, R. Wang, U. Ray, W. Gan, C. Li, G. Chen, B. Foster, T. Li and L. Hu, *Adv. Funct. Mater.*, 2020, **30**, 1910417.
55 G. Pan, F. Li, S. He, W. Li, Q. Wu, J. He, R. Ruan, Z. Xiao, J. Zhang and H. Yang, *Adv. Funct. Mater.*, 2022, **32**, 2200908.
56 N. Tang, Y. Jiang, K. Wei, Z. Zheng, H. Zhang and J. Hu, *Adv. Mater.*, 2024, **36**, 2309576.
57 C. Y. Wong, W. Y. Wong, K. S. Loh, W. R. W. Daud, K. L. Lim, M. Khalid and R. Walvekar, *Polym. Rev.*, 2020, **60**, 171–202.
58 Z. Zhou, J. Ma, K. Li, W. Zhang, K. Li, X. Tu, L. Liu, J. Xu and H. Zhang, *ACS Nano*, 2021, **15**, 8742–8752.
59 C. Geng, Y. Jiang, H. Bian and G. Huang, *Chem. Eng. J.*, 2024, **481**, 148757.
60 Z.-C. Li, W. Li, D.-X. Wang, R. Wang, A.-N. Tang and D.-M. Kong, *ACS Sustainable Chem. Eng.*, 2022, **10**, 10803–10815.
61 W. Wang, Z. Yu, F. K. Alsammarraie, F. Kong, M. Lin and A. Mustapha, *Food Hydrocolloids*, 2020, **100**, 105411.
62 P. Qu, M. Zhang, K. Fan and Z. Guo, *Crit. Rev. Food Sci. Nutr.*, 2022, **62**, 51–65.
63 Z. Bai, X. Wang, M. Zheng, O. Yue, M. Huang, X. Zou, B. Cui, L. Xie, S. Dong, J. Shang, G. Gong, A. M. Blocki, J. Guo and X. Liu, *Adv. Funct. Mater.*, 2023, **33**, 2212856.
64 B. M. Trinh, B. P. Chang and T. H. Mekonnen, *Prog. Mater. Sci.*, 2023, **133**, 101071.
65 J. Wang, D. J. Gardner, N. M. Stark, D. W. Bousfield, M. Tajvidi and Z. Cai, *ACS Sustainable Chem. Eng.*, 2018, **6**, 49–70.
66 W.-B. Zhao, Y. Wang, F.-K. Li, R. Guo, F.-H. Jiao, S.-Y. Song, S.-L. Chang, L. Dong, K.-K. Liu and C.-X. Shan, *Nano Lett.*, 2023, **23**, 11755–11762.
67 B. Maringgal, N. Hashim, I. S. M. A. Tawakkal and M. T. M. Mohamed, *Trends Food Sci. Technol.*, 2020, **96**, 253–267.
68 X. Gong, Q. Xu, X. Chen, F. Meng and H. Wang, *Carbon*, 2023, **210**, 118044.
69 S. Chen, Q. Zeng, X. Tan, M. Ye, Y. Zhang, L. Zou, S. Liu, Y. Yang, A. Liu, L. He and K. Hu, *Carbohydr. Polym.*, 2023, **314**, 120938.
70 D. Wang, C. Ding, Z. Feng, S. Ji and D. Cui, *Crit. Rev. Food Sci. Nutr.*, 2023, **63**, 1143–1154.
71 D. Góral, A. Marczuk, M. Góral-Kowalczyk, I. Koval and D. Andrejko, *Materials*, 2023, **16**, 780.

